The International Journal of Engineering and Science (IJES)
|| Volume || 8 || Issue || 9 Series I || Pages || PP 01-10 || 2019 ||
ISSN (e): 2319 – 1813 ISSN (p): 23-19 – 1805

Analysis of Permanent Magnet Synchronous Machine Considering Demagnetization Fault Based on Finite Element Method

Manel Fitouri, Yemna BenSalem[1], Mohamed Naceur Abdelkrim[1]
[1](*Research Laboratory Modelling, Analysis and Control of Systems (MACS) LR16ES22, National Engineering School of Gabes, Tunisia)*
Corresponding Author : Manel Fitouri

----------ABSTRACT----------
The paper study a novel approach which is developed and validated for Permanent Magnet Synchronous Motor (PMSM) motor with demagnetization fault. The analytical model is derived for the calculate the magnetic field distribution Permanent Magnet Synchronous Motor including with demagnetization fault to evaluate the back-electromotive force (EMF) induced and the electromagnetic torque in a Permanent Magnet (PM). The proposed model is used to analyze the effect of parameters (the magnetic field distribution, the back-EMF induced and the electromagnetic torque) by a finite element (FE) simulations.
Keywords *- Finite element method (FEM), Permanent Magnet Synchronous Motor (PMSM), Demagnetization fault.*

Date of Submission: 28-08-2019 Date of acceptance: 13-09-2019

I. INTRODUCTION

The introduction of the paper should explain the nature of the problem, previous work, purpose, and the contribution of the paper. The contents of each section may be provided to understand easily about the paper.
Permanent Magnet Synchronous Motors (PMSM) are widely used in high performance application such us automotive, appliances, medicine and aerospace because of their efficiency, reliability, multiple fields and high dynamic response performance [1]. As the use of this diversity applications, the diagnosis fault of PM machine becomes an important engineering field to enhance reliability and Keep the lifetime of drive systems [8], [11]. The most common PMSM fault types reported in industry are static and dynamic eccentricity, damaged bearings, demagnetization in rotor magnets, fault in connection of the stator windings and stator short-circuited turns.
Demagnetization fault is one of the most significant and frequently occurred type of faults in PM motor [7], [9], [12]. This type of fault is caused by the excessive field weakening the high temperature stress, the physical damage and the inverse magnetic field [6], [16], [18]. The literature has indicated that the effect of demagnetization fault can be investigate on the electromotive force (EMF) of the PM machine [17], [19]. In addition, this fault leads to the variations of the electromagnetic torque and the distribution of flux density [2].
The modeling and analysis of demagnetization fault have been discussed in literature. Many researchers have been studied demagnetization fault by using analytical methods based on Maxwell's equations [15], [19], magnetic equivalent circuits [2], [3] and permeance network methods [13]. For these reasons, the present paper studies the FE model of PMSM considering demagnetization fault. Initially, the analytical model is developed to determine the expression of the induced voltage and the torque according to the magnetic flux density.
In this study, the investigation is based on the finite element method (FEM) that is becoming progressively capable to analyze and simulate the demagnetization fault in each part of permanent magnet. To validate the analysis, a 2D-FEM simulation is used to verify the analytical model.

This paper is organized as follows. Section 1 has to do with an introduction. In section 2, we derived an analytical model for the electromagnetic torque, the back EMF induced and the flux density in a Permanent Magnet (PM) due to the demagnetization fault of PMSM. In section 3, we developed a FE model to verify the analytical model. Section 4 explains the model of the demagnetization fault of the machine. Section 5 is devoted to a conclusion for this paper.

II. ANALYTICAL MODEL

In this section, an analytical model is developed to exploit the simulation results of FEM. Fig.1 shows the simplified 2D model. The aim is pursued by evaluating the effect of the demagnetization fault on the induced voltage, the electromagnetic torque and the flux density [4], [5].

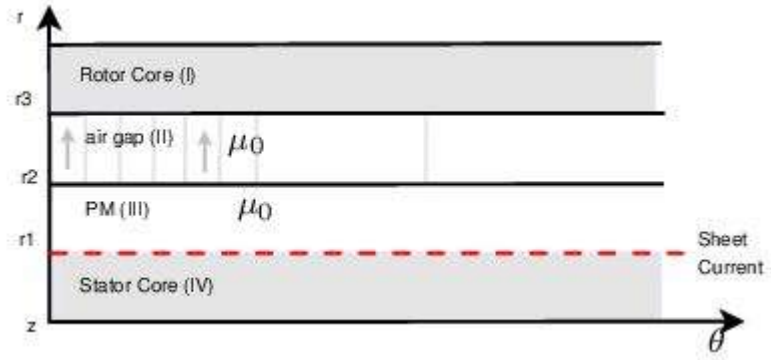

Fig.1. Simplified 2D model

The governing equation can be obtained using the Maxwell's equation [14], [20].
In the PM region,

$$div\, B = 0 \quad (1)$$

$$rot\, H = 0 \quad (2)$$

In the region II (air gap),

$$B_{II} = \mu_0 H_{II} \quad (3)$$

where B is the flux density, H is the field intensity and μ_0 is the permeability of the air.

To write the field equations in polar coordinates there are basically two regions:
In the air-gap as:

$$\nabla A_{II} = 0 \quad (4)$$

$$\frac{\partial^2 A_{II}}{\partial r^2} + \frac{1}{r}\frac{\partial A_{II}}{\partial r} + \frac{1}{r^2}\frac{\partial^2 A_{II}}{\partial \theta^2} = 0 \quad (5)$$

So, the general solution of (5) in the air gap region is written as

$$A_{II}(r,\theta) = \sum_{k=1}^{\infty} \left(\lambda_{II}.r^{kp} + \chi_{II}.r^{-kp}\right)\sin(kp\,\theta) \quad (6)$$

In the PM region,

$$B_{III} = \mu_0 \mu_r H_{III} + M \quad (7)$$

Where M is the magnetization of PMs and μ_r is the permeability of the air.
The magnetization of permanent magnet is given by

$$M(\theta) = M + \sum_{k=impair}^{\infty} \frac{2M}{k\pi}\sin(k\theta_0).\cos(kp\,\theta) \quad (8)$$

The field equations in polar coordinates in magnet regions is written as

$$\nabla A_{III} = \frac{1}{r}\frac{\partial M(\theta)}{\partial \theta} \quad (9)$$

$$\frac{\partial^2 A_{III}}{\partial r^2} + \frac{1}{r}\frac{\partial A_{III}}{\partial r} + \frac{1}{r^2}\frac{\partial^2 A_{III}}{\partial \theta^2} = \frac{1}{r}\frac{\partial M(\theta)}{\partial \theta} \quad (10)$$

The vector potential equations in magnet regions is given by

$$A_{III}(r,\theta)=\sum_{k=1}^{\infty}\left(\alpha_{III}.r^{kp}+\beta_{III}.r^{-kp}\right)\sin(kp\theta)+A_{III}^{p} \quad (11)$$

where

$$A_{III}^{p}(r,\theta)=\sum_{k=impair}\gamma.r\sin(kp\theta) \quad (12)$$

and

$$\gamma=-\frac{2pM}{(1-(kp)^2)\pi}\sin(k\theta_0) \quad (13)$$

Thus, the radial and tangential components of flux density in both regions (II and III) are

$$B_{II}^{r}(r,\theta)=\sum_{k=1}^{\infty}kp.\left(\lambda_{II}.r^{kp-1}+\chi_{II}.r^{-kp-1}\right)\cos(kp\theta) \quad (14)$$

$$B_{II}^{\theta}(r,\theta)=\sum_{k=1}^{\infty}kp.\left(\lambda_{II}.r^{kp-1}+\chi_{II}.r^{-kp-1}\right)\sin(kp\theta) \quad (15)$$

$$B_{III}^{r}(r,\theta)=\sum_{k=1}^{\infty}\left(kp.\left(\alpha_{III}.r^{kp-1}+\beta_{III}.r^{-kp-1}\right)-kp^2\delta_k\right)\cos(kp\theta) \quad (16)$$

$$B_{III}^{\theta}(r,\theta)=\sum_{k=1}^{\infty}\left(kp.\left(\alpha_{III}.r^{kp-1}+\beta_{III}.r^{-kp-1}\right)+p\delta_k\right)\sin(kp\theta) \quad (17)$$

Where

$$\delta_k=\frac{2M}{(1-(kp)^2)\pi}\sin(k\theta_0) \quad (18)$$

2.1 Electromagnetic torque expression

The electromagnetic torque expression is calculated using the Maxwell's stress tensor and it is expressed as follows

$$C_e=\frac{LR^2}{\mu_0}\int_0^{2\pi}B_{II}^{r}(r,\theta)B_{II}^{\theta}(r,\theta)\,d\theta \quad (19)$$

where L is the length of the machine and R is the radius of the integration surface.

2.2 Back Electromotive Force (EMF) expression

The expression of the induced back-EMF per phase is given as follow

$$e(t)=-N_s\frac{\partial\psi_{pm}}{\partial t}=-N_s\frac{\partial\theta}{\partial t}\frac{\partial\psi_{pm}}{\partial\theta}=-N_s\omega_r\frac{\partial\psi_{pm}}{\partial\theta} \quad (20)$$

where N_s is the number of turns per coil of one-phase winding and ω_r is the rotating speed of the rotor.

Therefore, the total fluxes ψ_{pm} linking all the coils of a phase are calculated as follow:

$$\psi_{pm}=\int_0^{2\pi}B_{II}^{r}(r,\theta)\,d\theta \quad (21)$$

The analytical magnetic flux density distributions have been used to calculate the important quantities, such as electromagnetic torque and the back-EMF induced. We derived the analytical solution for magnetic flux distribution in order to show the effects of demagnetization fault in permanent magnet on back-EMF and electromagnetic torque waveforms.

The preferred validation analytical model is provided by a FE model of a PM model employing the to study the effect of the motor performance on the demagnetization fault. In this case, the analytical model is carried out based on a FE solutions as described in the section 3.

III. FINITE ELEMENT MODEL OF PMSM

The FEM is a computer based numerical technique to calculate the parameters of the electromagnetic devices. It can be used to calculate the flux density, the flux linkages, the inductance, the torque, the induced EMF etc. A FEM, which addresses dynamic material properties of the magnets and yet can be implemented readily in the software, is presented to find the parameters of the magnetization circuit.

The magnetic field distribution inside the machine is calculated using the FEM. This distribution can be used to calculate other properties such as the induced voltage of the machine. Also, it provides detailed information about the nonlinear effects of the machine (based on its geometry and material properties). The finite element analysis is utilized to verify the analytical expressions, as well as to determine the electromagnetic torque and the induced voltage generated by demagnetization fault.

Fig.2 shows the FE model of a the PMSM which is simulated in 2D-FE environment, employed to confirm the validity of the analytical method. Its main specifications are listed in Table.1.

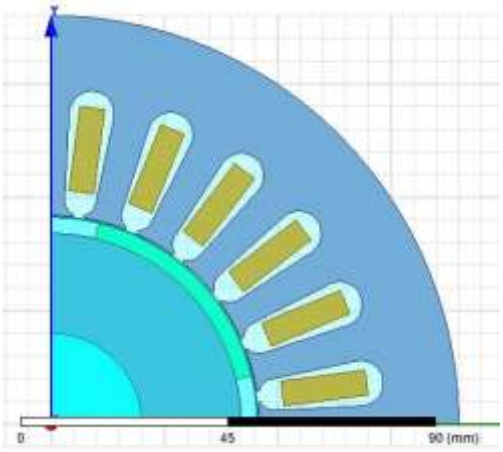

Fig.2. Finite Element Model of PMSM

Simulation results of the PMSM in healthy operating conditions are depicted in **Fig.3.**

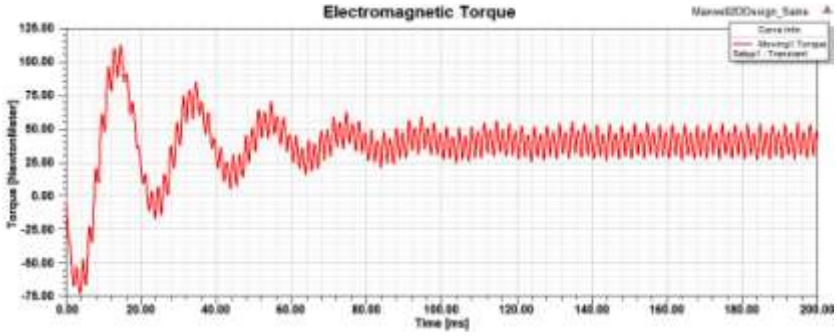

a. Electromagnetic torque

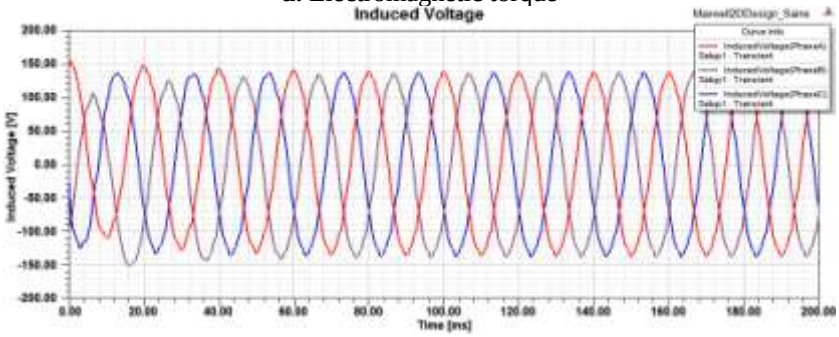

b. Stator induced voltage

Fig.3. Simulation results of PMSM in normal operating conditions.

Analyzing the flux distributions density in the machine's core reaches satisfactory values without any highly saturated regions as shown in **Fig.4.**

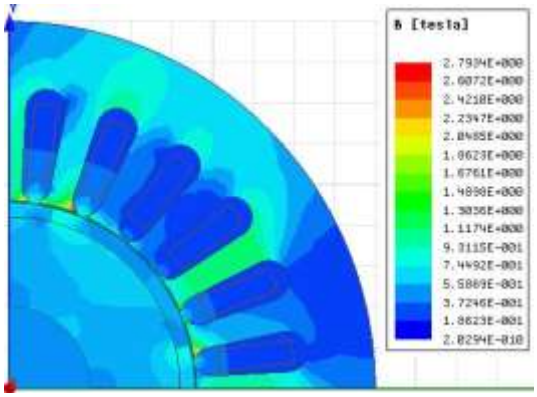

Fig.4. Flux distributions of PMSM in healthy case.

IV. DEMAGNETIZATION FAULT MODELING OF PMSM

In this study, the effect of electromagnetic field of the PMSM for the demagnetization fault is presented. FEM is the main technique for calculating the magnetic flux density distributions in the machine under different rotor fault conditions. In this section, a comparison of magnetic flux density distribution for a machine with a healthy and a faulty rotor are presented.

Following, the demagnetization fault was modeled by cutting 10, 20 and 50 % of part of the magnet, shown in **Fig.5**.

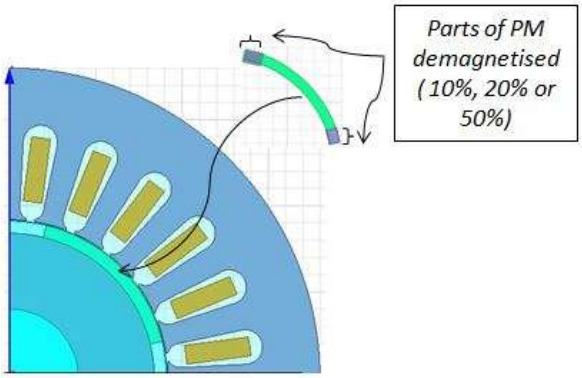

Fig.5. Faulty machine with demagnetization fault

Fig.6 and **Fig.7** show the magnetic flux density distribution in the PMSM and in permanent magnet under different fault conditions.

The distribution of the magnetic flux density for a faulty machine is shown in **Fig.6** at 0.2 [s].

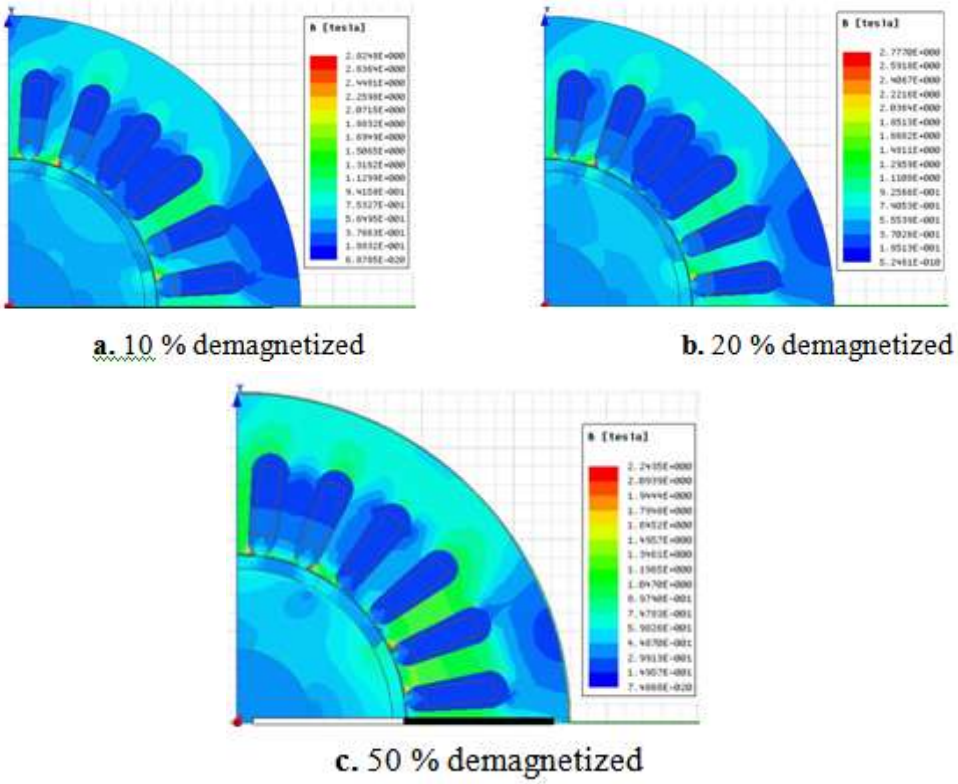

Fig.6. Magnetic flux density distribution of PMSM under different fault conditions.

In **Fig.6**, the demagnetization fault of the magnets, according to 2D model, is shown for the four fault conditions. It shows that under fault conditions, the risk of demagnetization is actually low, contrary when the demagnetized part of permanent magnet increase.

Fig.7.a, **Fig.7.b** and **Fig.7.c** illustrate the situation under the different fault conditions. The distribution of flux density in PM shows that the outer corners of the magnets may be susceptible to demagnetization under these conditions.

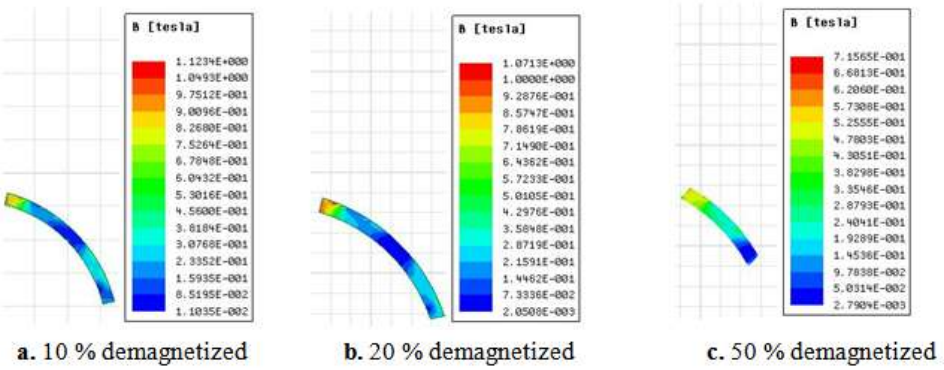

Fig.7. The distribution of flux density in PM under different fault conditions.

The three curves compare favorably with different fault conditions are shown in **Fig.8**. During the three case of demagnetized fault (10 %, 20 % and 50 % of demagnetization fault), the torque ripple decreases. It is obvious that as the demagnetized part increases, the torque ripple deteriorates.

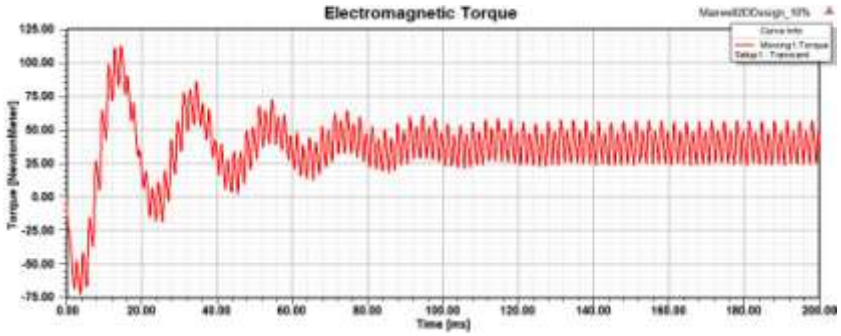

a. 10 % demagnetized

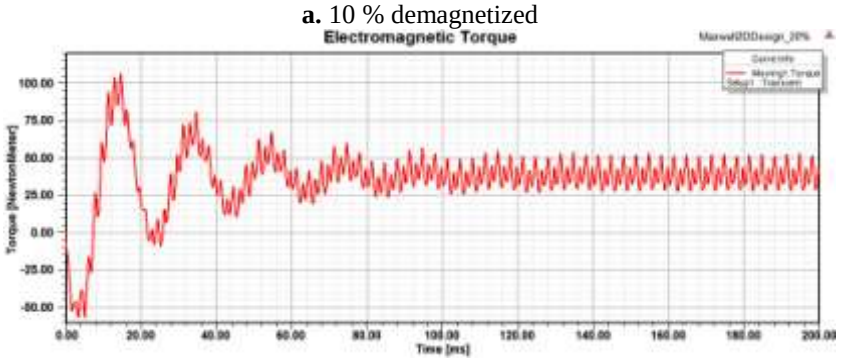

b. 20 % demagnetized

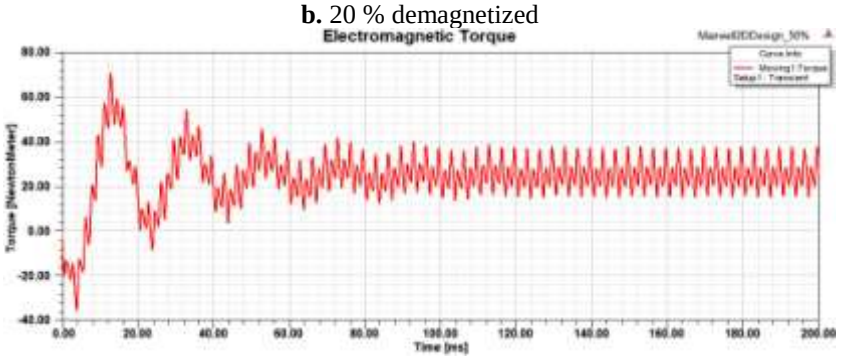

c. 50 % demagnetized

Fig.8. Simulation Results of electromagnetic torque under different fault conditions.

Fig.9 shows a comparison of the results with different fault conditions for the induced voltage according to the demagnetization fault. For more clearly comparison of the results, the peak value of the induced voltage results are confirmed about 2 % by comparing with different fault conditions results. It can be seen that the curves of the induced voltage according to demagnetization fault are not a pure sinusoidal waveform and are deformed with the increase of the demagnetized part.

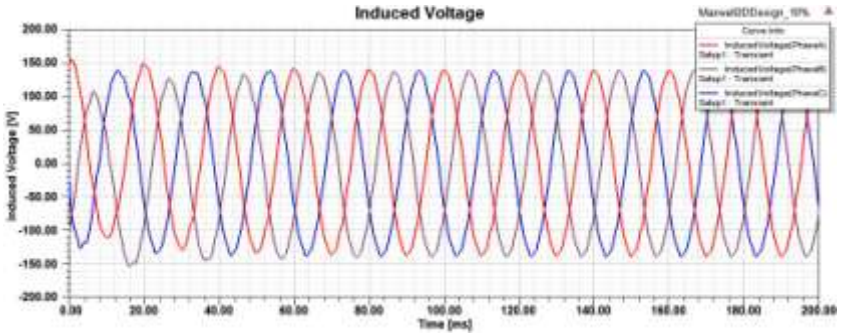

a. 10 % demagnetized

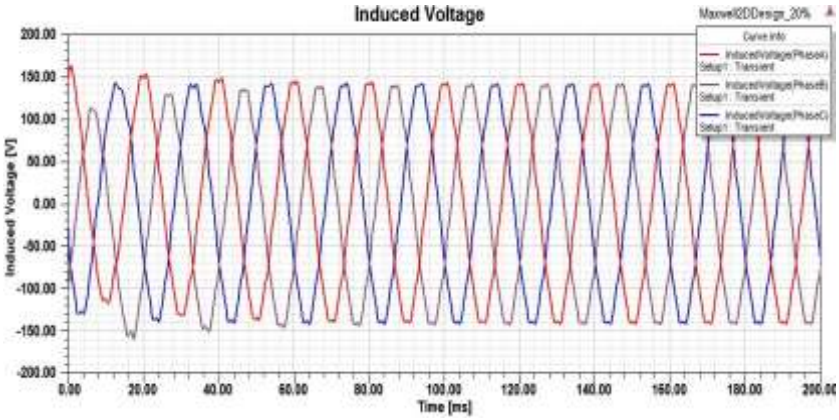

b. 20 % demagnetized

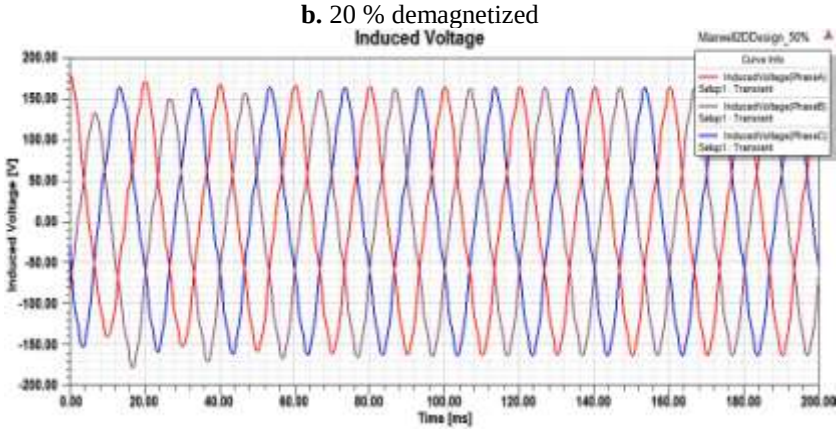

c. 50 % demagnetized

Fig.9. Simulation Results of stator induced voltage under different fault conditions.

Fig.10 presents the influence of various levels of demagnetization faults on the induced voltage and the torque ripple while the various levels of demagnetization faults vary from 10 %, 20 % and 50 % obtained with FE simulations. It can be seen in **Fig.10.a** that the induced voltage increase with the increase of the percentage of the demagnetized parts.

Nevertheless, as it can be observed in **Fig.10.b**, the value of the torque is strongly influenced by the different cases of demagnetized fault.

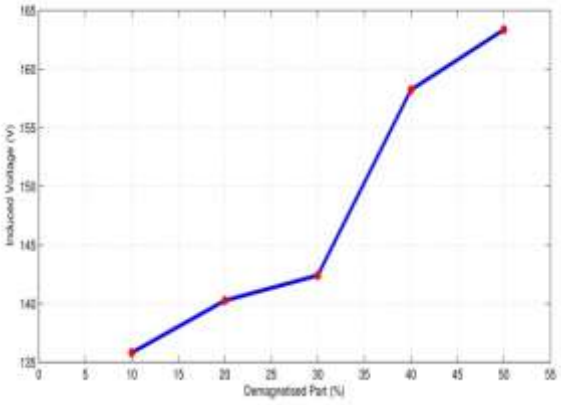

(a)

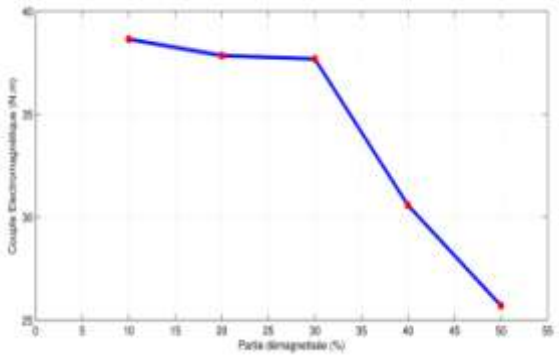

(b)

Fig.10. The effect of the induced voltage and the electromagnetic torque for several of demagnetized fault predicted by the FEM

V. CONCLUSION

On the basis of analytical magnetic-field computation techniques, the analytical model for a PMSM considering demagnetization fault have been developed. The results of the nonlinear FEM are used to confirm the validity of the analytical solutions for the electromagnetic torque, the induced voltage and the magnetic field. The results under different conditions obtained by the FEM Software are presented and analyzed.

ACKNOWLEDGEMENTS

This work was supported by the Ministry of the Higher Education and Scientific Research in Tunisia.

Table 1. Specification Adopted of PMSM.

Permanent Magnet Synchronous Motor	
Parameters	**Values**
Number of poles	4
Output power	15 Kw
rated voltage	127 V
Speed	1500 rpm
Frequency	50 Hz
Rotor inner diameter	40 mm
Length of Rotor	101 mm
Stator outer diameter	180 mm
Stator inner diameter	90 mm
Length of Stator Core	101 mm

REFERENCES

[1]. C M Apostoaia, Multi-domain system models integration for faults detection in induction motor drives, International Conference on IEEE Electro/Information Technology (EIT), 2014.

[2]. G Choi and T M Jahns, Post-demagnetization characteristics of permanent magnet synchronous machines, in IEEE Transactions on Energy Conversion Congress and Exposition (ECCE), 2015, 1781-1788.

[3]. N Bianchi and T M Jahns, Design analysis and control of interior PM synchronous machines, in IEEE-IAS Electrical Machines Committee, 2004.

[4]. K H Shin, H Il Park, H W Cho and J Y Choi, Analytical Calculation and Experimental Verification of Cogging Torque and Optimal Point in Permanent Magnet Synchronous Motors, in IEEE Transactions on Magnetics, 53(6), 2017.

[5]. J M Kim, J Y Choi, S H Lee and S M Jang, Characteristic analysis and experiment of surface-mounted type variable-flux machines considering magnetization/demagnetization based on electromagnetic transfer relations, in IEEE Transactions on Magnetics, 50(11), 2014.

[6]. Z Hou, J Huang, H Liu, Z Liu, M Ye and J Yang, No-load losses based method to detect demagnetisation fault in permanent magnet synchronous motors with parallel branches, IET Electric Power Applications, 11(3), 2017.

[7]. G H Kang, J Hur, H Nam, J P Hong and G T Kim, Analysis of irreversible magnet demagnetization in line-start motors based on the finite-element method, in IEEE Transactions on Magnetics, 39(3), 2003.

[8]. S S Moosavi, A Djerdir, Y A Amirat and D A Khaburi, Demagnetization fault diagnosis in permanent magnet synchronous motors: A review of the state-of-the-art, in Elsevier Journal of Magnetism and Magnetic Materials, 391, 2015.

[9]. R Z Haddad and E G Strangas, Fault detection and classification in permanent magnet synchronous machines using Fast Fourier Transform and Linear Discriminant Analysis, in IEEE International Symposium on Diagnostics for Electric Machines, Power Electronics and Drives (SDEMPED), 2013, 99 - 104.

[10]. J H Yoo, D H Hwang and T U Jung, Irreversible Demagnetization Fault Diagnosis of Permanent Magnet Synchronous Motor for Electric Vehicle, in IEEE on Vehicle Power and Propulsion Conference (VPPC), 2015 , 1 - 4.

[11]. M Cheng, J Hang and J Zhang, Overview of fault diagnosis theory and method for permanent magnet machine, in Chinese Journal of Electrical Engineering, 1(1), 2015.
[12]. J Faiz and E Mazaheri-Tehrani, Demagnetization Modeling and Fault Diagnosing Techniques in Permanent Magnet Machines Under Stationary and Nonstationary Conditions: An Overview, in IEEE Transactions on Industry Applications, 53(3), 2017.
[13]. F J Ahmed, A Djerdir and A Miraoui, Identification of demagnetization faults in a permanent magnet synchronous machine by permeance network, in The international journal for computation and mathematics in electrical and electronic engineering, 28(6), 2009.
[14]. J A Farooq and A Djerdir and A Miraoui, An Inverse Problem Methodology to Analyze Demagnetization Phenomenon in Permanent Magnet Machines, IEEE Conference on Electromagnetic Field Computation, 2006, 41-41.
[15]. P Liang and F Chai and Y Bi and Pei, Yulong and S Cheng, Analytical model and design of spoke-type permanent-magnet machines accounting for saturation and nonlinearity of magnetic bridges, in Elsevier Journal of Magnetism and Magnetic Materials, 417, 2016.
[16]. S Ruoho, J Kolehmainen, J Ikaheimo and A Arkkio, Interdependence of demagnetization, loading, and temperature rise in a permanent-magnet synchronous motor, in IEEE Transactions on Magnetics, 46(3), 2010.
[17]. K C Kim, S B Lim, D H Koo and Ju Lee, The shape design of permanent magnet for permanent magnet synchronous motor considering partial demagnetization, in IEEE Transactions on Magnetics, 42(10), 2010.
[18]. K T Kim, Y S Lee and J Hur, Transient analysis of irreversible demagnetization of permanent-magnet brushless DC motor with interturn fault under the operating state, in IEEE Transactions on Industry Applications, 50(5), 2014.
[19]. J A Farooq, A Djerdir and A Miraoui, Analytical modeling approach to detect magnet defects in permanent-magnet brushless motors, in IEEE Transactions on Magnetics, 44(12), 2008.
[20]. Jawad Ahmed Farooq. Etude du problème inverse en électromagnétisme en vue de la localisation des défauts de désaimantation dans lesactionneursàaimantspermanents. PhD thesis, 2008.

Karim Usman" Securing Data on Transmission from Man-In-The-Middle Attacks Using Diffie Hell-Man Key Exchange Encryption Mechanism" The International Journal of Engineering and Science (IJES), 8.9 (2019): 01-10